

The elastic moduli of oriented tin oxide nanowires

Sven Barth^{1,2,4}, Catalin Harnagea¹, Sanjay Mathur^{2,3} and Federico Rosei^{1,4}

¹ INRS-Énergie, Matériaux et Télécommunications, Université du Québec, J3X 1S2 Varennes, Canada

² Institute of Inorganic Chemistry, University of Wuerzburg, D-97074 Wuerzburg, Germany

³ Institute of Inorganic Chemistry, University of Cologne, Cologne, Germany

E-mail: sbarth76@gmail.com and rosei@emt.inrs.ca

Received 10 November 2008, in final form 21 December 2008

Published 25 February 2009

Online at stacks.iop.org/Nano/20/115705

Abstract

Tin oxide nanowires (NWs) exhibit interesting electronic properties, which can be harnessed for applications in nanoelectronic devices and sensors. Oriented single crystalline tin oxide NWs were grown at 45° from a titanium dioxide substrate. Their elastic properties were investigated in a two-point geometry using an atomic force microscope (AFM) coupled with a scanning electron microscope under ultrahigh vacuum conditions. Young's modulus was calculated by bending individual NWs and measuring the force exerted on the AFM tip during force–displacement measurements. For the NWs investigated, having radial dimensions below 45 nm and length up to 1.2 μm, we found an average value of 100 ± 20 GPa, which is below the theoretical predictions calculated for different SnO₂ single crystal orientations, yet consistent with the indentation moduli of nanobelts. Finally, we discuss the effects of the nanowire–cantilever configuration on the measured Young's modulus.

1. Introduction

Anisotropic inorganic nanostructures such as nanowires (NWs) continue to be the subject of intense research efforts due to the directional mobility of charge carriers, the single crystalline properties and the high aspect ratio, which have led to several interesting phenomena with opportunities for novel applications [1–4].

Several approaches were recently used to determine the mechanical properties of inorganic high aspect ratio nanostructures [5]. These investigations are essential for practical implementation of such building blocks as active or passive components in nanodevices. Nanoscale mechanical failure could lead to malfunction or destruction of an entire integrated circuit; it is therefore one of the aspects to be explored for the fabrication of reliable devices with long-term stable performance. Among the methodologies available, the most important techniques used to evaluate their Young's modulus are alternating electric field-induced excitation (which allows to monitor resonance frequencies) [6] and quasi-static bending of one-dimensional structures by atomic force

microscopy (AFM) [7]. Contact resonance AFM [8] and nanoindentation experiments [9] were successfully used to investigate the mechanical properties of nanowires (NWs). Bending experiments could either be performed in three-point geometry with two ends of a nanowire bridging a predefined gap [10] or in two-point geometry on oriented wires [11]. The observed data for fracture strength of group 4 semiconductors ranges from 15% up to the ultimate limit of the theoretical strength, which was attributed to the density of defects within the nanostructure [12].

One-dimensional SnO₂ semiconductors can be used as active components in nanoelectronic systems and resistance-based gas sensors [13]. Recently, we investigated the electrical properties of SnO₂ NWs and their response towards gaseous species such as water, carbon monoxide and nitrogen dioxide [14]. Gas sensing without external heaters was reported for SnO₂ nanowire-based devices, which used the self-heating effect to achieve the appropriate sensing temperature [15]. In addition, fully transparent transistors based on SnO₂ NWs on glass substrates were described in the literature [16]. However, the key factor for the fabrication of multifunctional (simultaneously electronic and sensor) devices on flexible substrates remains the elastic modulus of individual NWs.

⁴ Authors to whom any correspondence should be addressed.

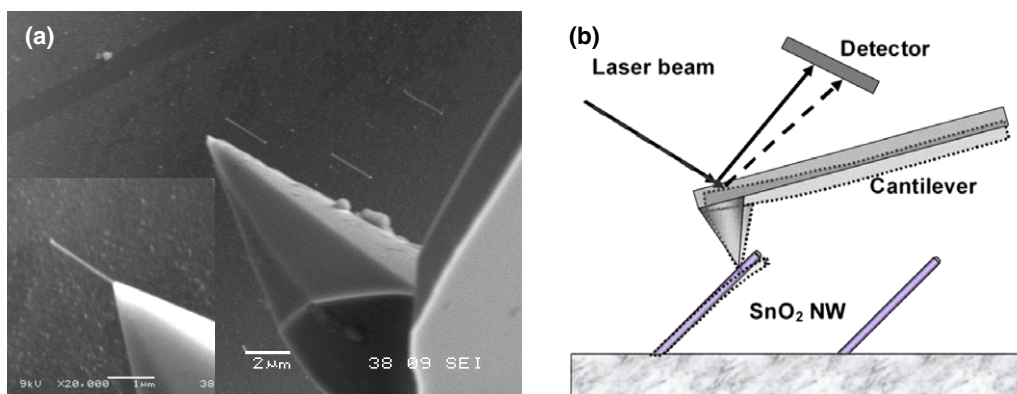


Figure 1. (a) SEM image of oriented tin oxide nanowires and AFM tips used to probe selected individual nanostructures as demonstrated in the inset. (b) Scheme of the cantilever–nanowire geometry in the performed experiments. The viewing direction is parallel to the substrate.

Indeed, knowledge about the elastic behavior of the NWs (in terms of deformation under an applied stress) is crucial in designing reliable, long lasting, bendable devices and assessing their endurance to nanoscale mechanical failure. Here we investigate the mechanical properties of single SnO₂ NWs by combining simultaneous AFM measurements and scanning electron microscopy (SEM) imaging under ultrahigh vacuum (UHV) conditions.

2. Experimental section and results

Single crystalline (301)-oriented SnO₂ nanostructures were grown at an angle of 45° with respect to the substrate by molecule-based gold catalyzed approach at 700 °C substrate temperature on (001) TiO₂ surfaces, as described in detail elsewhere [17]. Gold colloid solutions with mean particle size of 20 nm (Sigma Aldrich) were spin coated on the substrates and enabled the growth of SnO₂ NWs with diameters in the range of 42 ± 3 nm. Mechanical measurements were performed in a JEOL 4500 UHV-AFM/STM instrument equipped with an SEM column and secondary electron detector. SEM imaging was used to guide the cantilever to appropriate positions on the selected nanowires, as shown in figure 1(a). Since the SEM images are taken at an angle of approximately 45° with respect to the sample surface and AFM tip axis (fixed experimental geometry), the images are slightly distorted. A scheme showing the cantilever to nanowire geometry in these investigations is displayed in figure 1(b). After positioning the tip, standard force–displacement curves were recorded, by averaging over 128 individual bending cycles. We performed the measurements on 13 individual NWs, at different positions along the NW axis. The photodiode signal was calibrated by performing the force measurements above the hard substrate (single crystalline TiO₂). AFM silicon cantilevers (NSC 36, from Mikromasch) with nominal spring constants (k_c) between (0.5–2.4 N m⁻¹) were used in the experiments. The spring constant of each cantilever was estimated by comparing the cantilever's first resonance frequency (f_1) with the data sheet provided by the supplier, knowing that k_c and f_1 are directly related.

In AFM-based experiments, tip–nanowire interactions are complex and for reliable experimental studies the presence

of friction (due to slipping) as well as van der Waals forces between the nanowire and tip should be taken into account [18].

While using SEM to monitor the NW being bent by the AFM tip, sometimes lateral slipping is observed and related kinks appear in the force curve. When such events occurred, we adjusted the tip position with respect to the nanowire using the JEOL operating software until the force–displacement data is corrected as shown in figure 2. However, possible continuous slipping of the tip along the tilted NW would result in a friction force which could induce a systematic error in the measurements. As the friction force is directed along the NW, the component perpendicular to the substrate will contribute to the normal force sensed by the cantilever. Since this component is proportional to the friction force by the friction coefficient, the slope of the force curve will be affected. The direction of the friction force depends on the relative movement between the two surfaces, this means that the load/unload force curves will be different by twice the friction force. The latter therefore will exhibit a hysteretic behavior. We observed such hysteresis in the force data, yet an estimation of the friction coefficient was not possible due to the variability in the hysteresis width, possibly caused by the specific tip–NW contact geometry (which in turn depends on the contact angle). Therefore, in our estimation of the Young modulus we used only force curves for which the load/unload directions matched closely. Additionally, the component of the friction force parallel to the cantilever axis results in its buckling, possibly contributing to the measured force. While strictly speaking we should only consider in our calculation the force perpendicular to the cantilever for the reasons mentioned above (complex contact geometry, variable contact angle, and buckling contribution), we considered in this first report the force data as measured by the cantilever. We limited the NW bending to <200 nm, while most of the measurements performed in the 100–150 nm range did not exhibit noticeable signs of kinks in the load–unload data. Monitoring the NW–tip interaction is mandatory to relate the measurement conditions to data obtained. To achieve this, we have taken into account the following factors: first, to assess the NW's dimensions, we have carefully considered the 45° viewing

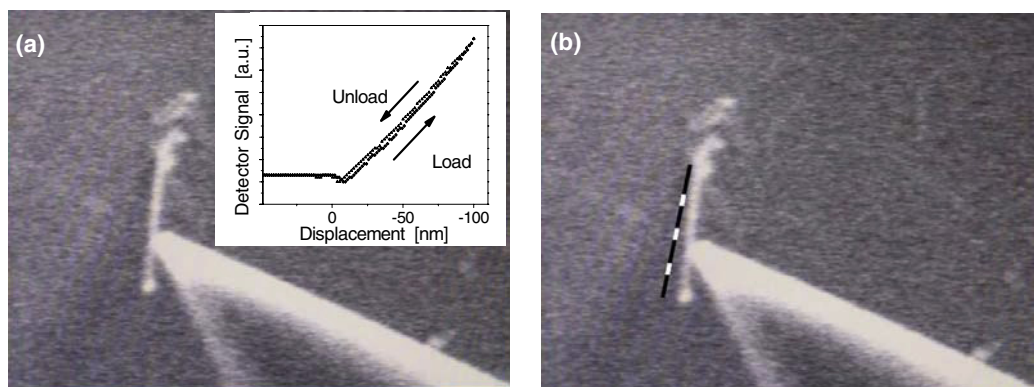


Figure 2. Bending of an individual tin oxide nanowire, monitored by SEM and recorded using AFM: (a) the NW bent by the tip during a force measurement. (b) The tip in contact with the NW, before and after the measurement. The dashed line illustrates the NW at maximum flexion (drawn by superposing with image (a)). The inset in (a) shows the force–displacement curve recorded. A slight hysteresis is observed, associated to cantilever buckling caused by friction.

angle of SEM images, as well as the NW orientation with respect to the substrate. Second, since SnO_2 is a large bandgap semiconductor, charging effects in SEM imaging could lead to blurring of the feature images and affect the Young modulus values in figure 3(b). By comparing the wire diameter with the size of the catalytic gold nanoparticles and with our TEM results [17], we insured that the charging effect does not lead to an overestimation of the radial dimensions (and therefore to an underestimation of the Young's modulus), however slight diameter variations could cause a spread of the calculated values.

To determine the mechanical properties of the SnO_2 nanowires we used the linear-elastic force–displacement (F – d) curves without damaging or modifying the nanostructure, and applied the elastic beam bending theory to each NW. The slope s_{comb} of the linear region of the F – d curves recorded while bending a NW is used to calculate the spring constant of the wire k_w , employing a formula that has been previously applied to calibrate cantilevers using microfabricated elastic devices [19]:

$$k_w = k_{\text{Cant}} / (s / s_{\text{comb}} - 1).$$

Here, s is the slope of the F – d curve recorded against the hard substrate surface, i.e. the sensitivity of the z -displacement detection system. Using the spring constant of the bended region of the NW, k_w , we determine the Young's modulus E of the SnO_2 nanowires using the well-known result from elastic beam theory [20]

$$E = k_w \frac{64L^3}{3\pi d^4}$$

here we considered the NW a cylinder with diameter d and length L , the latter being the distance from the contact point to the fixed base of the NW (i.e. the region of the NW exposed to the force applied by the AFM tip). Obviously, the errors in determining the NW dimensions play a crucial role in the accuracy of the measured Young modulus.

The experimental results are summarized in figure 3. Figure 3(a) shows as an example the results for a typical NW. The Young modulus, estimated as described above is 110 ± 10 GPa. The error, close to 10%, can

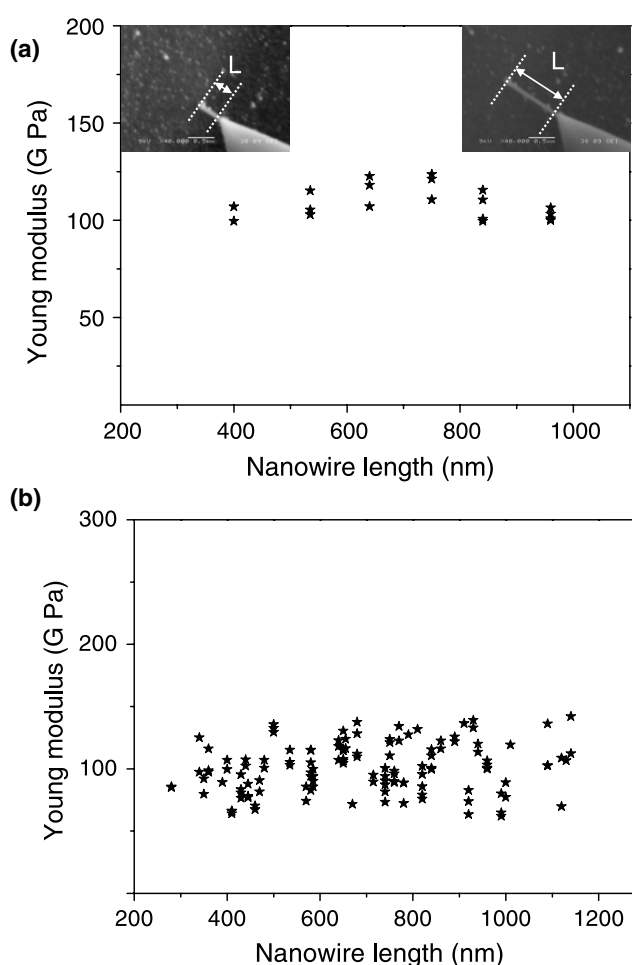


Figure 3. Calculated E -modulus versus nanowire length of single crystalline SnO_2 nanowires. The NW length was determined as shown in the SEM images (insets, the scale bars represent $0.5 \mu\text{m}$). Data were obtained for (a) an individual specimen and (b) 13 NWs.

be attributed to measurement variability while probing freestanding nanostructures as explained above, as well as to the anisotropy and nonlinear behavior of the NW. The data for all the investigated individual NWs shown in figure 3(b) revealed a Young modulus of 100 ± 20 GPa. The standard

deviation, 20% of the average value, is fairly large and can be explained as follows: the SnO₂ NWs being single crystalline the effective Young modulus intervening in the above equation is anisotropic, spanning for bulk tetragonal tin oxide from 174 to 368 GPa [21], therefore by over a factor of 2. Since the NWs grow highly oriented from the substrate but the exact epitaxial relationship at the interface is still under debate [17b] the obtained data cannot be compared to a specific orientation-dependent value. Additionally, knowing that the stress and strain induced during the measurements are mainly localized near the base of the wire, it follows that the mechanical constraint at the interface between the NW and substrate again plays a significant role in the elastic deformation of the NW. While the structure determination by TEM and electron diffraction showed clearly the single crystalline nature of the NWs, a slight oxygen deficiency (well known to occur in vapor-grown oxides) could also alter the mechanical properties of the oxide NWs.

The values obtained in the present study are comparable to indentation modulus reported in the literature for SnO₂ nanobelts (150 GPa in [18a] and 60 GPa in [18b]), however, to the best of our knowledge no Young moduli for 1D SnO₂ nanostructures are available. These values, well below the bulk single crystalline levels, confirm somewhat previous reports of reduced elastic modulus of NWs with decreasing diameter, a size-dependence attributed to surface stress and surface elasticity [22]. The induced stress and strain is mainly localized near the base of the wire, where a broadening of the radial dimension is observed [22]. Therefore, our results together with [23] contradict recent simulations for ZnO nanobelts, predicting increasing elastic modulus with reducing dimensions [24]. The low values obtained for the elastic moduli need therefore further investigations both theoretically and experimentally to evaluate the finite size-effects in nanoscale SnO₂.

3. Conclusions

In summary, we have investigated the mechanical moduli of (301)-oriented single crystalline SnO₂ NWs with radial dimensions below 45 nm. The AFM force–displacement measurements on aligned NWs grown at a 45° angle with respect to the substrate showed a Young's modulus of 100 ± 20 GPa, comparable to that reported for SnO₂ nanobelts. However the data from force–displacement curves were still below the values of SnO₂ bulk material, contradicting recent theoretical work. Size-dependent mechanical properties of SnO₂ NWs and verification of the results presented herein will be evaluated in future studies based on three-point bending experiments in the NW diameter range 20–500 nm. These nanostructures can be synthesized by a molecule-based approach as described in literature [17a].

Acknowledgments

Thanks are due to the German Science Foundation (DFG) for supporting this work in the frame of the priority program on nanomaterials—Sonderforschungsbereich 277— at the Saarland University, Saarbruecken, Germany. We

acknowledge financial support from the Bavaria–Quebec collaborative initiative, which enabled this collaboration. FR is grateful to the Canada Research Chairs program for partial salary support and thanks NSERC and the CFI-IOF for operating funds.

References

- [1] Cui Y, Wei Q Q, Park H K and Lieber C M 2001 *Science* **293** 1289
Huang M H, Mao S, Feick H, Yan H, Wu Y, Kind H, Weber E, Russo R and Yang P 2001 *Science* **292** 1897
- [2] Presley R E, Munsee C M, Park C H, Hong D, Wagner J F and Keszler D F 2004 *J. Phys. D: Appl. Phys.* **37** 1624
Barth S, Estrade S, Hernandez-Ramirez F, Peiro F, Arbiol J, Romano-Rodriguez A and Mathur S 2009 *Cryst. Growth Des.* **9** 1077
Vayssieres L, Sathe C, Butorin S M, Shuh D K, Nordgren J and Guo J 2005 *Adv. Mater.* **17** 2320
Vayssieres L 2007 *Appl. Phys. A* **89** 1
- [3] Tian Z R R, Voigt J A, Liu J, McKenzie B, McDermott M J, Rodriguez M A, Konishi H and Xu H F 2003 *Nat. Mater.* **2** 821
Mathur S, Barth S, Werner U, Hernandez-Ramirez F and Romano-Rodriguez A 2008 *Adv. Mater.* **20** 1550
Woodruff J H, Ratchford J B, Goldthorpe I A, McIntire B C and Chidsey C E D 2007 *Nano Lett.* **7** 1637
- [4] Rosei F 2004 *J. Phys.: Condens. Matter* **16** S1373
- [5] Yu M F, Lourie O, Dyer M J, Moloni K, Kelly T F and Ruoff R F 2000 *Science* **287** 637
Zheng D J and Zheng Q S 2007 *Phys. Rev. B* **76** 075417
Zhu Y, Ke C and Espinosa H D 2007 *Exp. Mech.* **47** 7
Wong E W, Sheehan P E and Lieber C M 1997 *Science* **277** 1971
Poncharal P, Wang Z L, Ugarte D and De Heer W A 1999 *Science* **283** 1513
Heidelberg A, Ngo L T, Wu B, Phillips M A, Sharma S, Kamins T I, Sader J E and Boland J J 2006 *Nano Lett.* **6** 1101
- [6] Nam C Y, Jaroenapibal P, Tham D, Luzzi D E, Evoy S and Fischer J E 2006 *Nano Lett.* **6** 153
Huang Y, Bai X and Zhang Y 2006 *J. Phys.: Condens. Matter* **18** L117
Wang Z L, Dai Z R, Gao R P, Bai Z G and Gole J L 2000 *Appl. Phys. Lett.* **77** 3349
- [7] Hoffmann S, Östlund F, Michler J, Fan H J, Zaccharias M, Christiansen S H and Ballif C 2007 *Nanotechnology* **18** 205503
- [8] Stan G, Ciobanu C V, Parthagal P M and Cook R F 2007 *Nano Lett.* **7** 3691
- [9] Feng G, Nix W D, Yoon Y and Lee C J 2006 *J. Appl. Phys.* **99** 074304
Ni H and Li X 2006 *Nanotechnology* **17** 3591
- [10] Wu B, Heidelberg A and Boland J J 2005 *Nat. Mater.* **4** 525
- [11] Song J, Wang X, Riedo E and Wang Z L 2005 *Nano Lett.* **5** 1954
- [12] Petersen K E 1982 *Proc. IEEE* **70** 420
Hofman S, Utke I, Moser B, Michler J, Christiansen S H, Schmidt V, Senz S, Werner P, Gösele U and Ballif C 2006 *Nano Lett.* **6** 622
Ngo L T, Almecija D, Sader J E, Daly B, Petkov N, Holmes J D, Erts D and Boland J J 2006 *Nano Lett.* **6** 2964
- [13] Batzill M and Diebold U 2005 *Prog. Surf. Sci.* **79** 47
Hernandez-Ramirez F, Rodriguez J, Casals O, Russinyol E, Vila A, Romano-Rodriguez A, Morante J R and Abid M 2006 *Sensors Actuators B* **118** 198
- [14] Hernandez-Ramirez F, Barth S, Tarancon A, Casals O, Pellicer E, Rodriguez J, Romano-Rodriguez A, Morante J R and Mathur S 2007 *Nanotechnology* **18** 424016

- Mathur S and Barth S 2008 *Z. Phys. Chem.* **222** 307
- Hernandez-Ramirez F, Tarancon A, Casals O, Pellicer E, Rodriguez J, Romano-Rodriguez A, Morante J R, Barth S and Mathur S 2007 *Phys. Rev. B* **76** 085429
- Hernandez-Ramirez F *et al* 2007 *Nanotechnology* **18** 495501
- Hernandez-Ramirez F, Tarancon A, Casals O, Rodriguez J, Romano-Rodriguez A, Morante J R, Barth S, Mathur S, Choi T Y, Poulidakos D, Callegari V and Nellen P M 2006 *Nanotechnology* **17** 5577
- [15] Prades J D, Jimenez-Diaz R, Hernandez-Ramirez F, Barth S, Cicera A, Mathur S, Romano-Rodriguez A and Morante J R 2008 *Appl. Phys. Lett.* **93** 123110
- [16] Dattoli E N, Wan Q, Guo W, Chen Y, Pan X and Lu W 2007 *Nano Lett.* **7** 2463
- [17a] Mathur S, Barth S, Shen H, Pyun J-C and Werner U 2005 *Small* **1** 713
- [17b] Mathur S and Barth S 2007 *Small* **3** 2070
- [18a] Zheng Y, Geer R E, Dovidenko K, Kopycinska-Müller M and Hurley D C 2006 *J. Appl. Phys.* **100** 124308
- [18b] Mao S X, Zhao M and Wang Z L 2003 *Appl. Phys. Lett.* **83** 993
- [19] Cumpson P J, Hedley J and Zhdan P 2003 *Nanotechnology* **14** 918
- [20] Sarid D 1991 *Scanning Force Microscopy* (Oxford: Oxford University Press)
- [21] Li H and Bradt R C 1991 *J. Am. Ceram. Soc.* **94** 1053
- [22] Chen C Q, Shi Y, Zhang Y S, Zhu J and Yan Y J 2006 *Phys. Rev. Lett.* **96** 075505
- Miller R E and Shenoy V B 2000 *Nanotechnology* **11** 139
- Cuenot S, Fretigny C, Demoustier-Champagne S and Nysten B 2004 *Phys. Rev. B* **69** 165410
- Lucas M, Mai W, Yang R, Wang Z L and Riedo E 2007 *Nano Lett.* **7** 1314
- [23] Chen C Q and Zhu J 2007 *Appl. Phys. Lett.* **90** 043105
- [24] Kulkarni A J, Zhou M and Ke F J 2005 *Nanotechnology* **16** 2749